https://doi.org/10.1093/plphys/kiac234 PLANT PHYSIOLOGY 2022: 189: 2029–2043

Plant Physiology®

Research Article

Consecutive action of two BAHD acyltransferases promotes tetracoumaroyl spermine accumulation in chicory

Guillaume Bernard [1], Julie Buges,[1] Marianne Delporte [1], Roland Molinié [2], Sébastien Besseau [3], Alain Bouchereau [4], Amandine Watrin,[1] Jean-Xavier Fontaine [2], David Mathiron [5], Solenne Berardocco [4], Solène Bassard [2], Anthony Quéro,[2] Jean-Louis Hilbert [1], Caroline Rambaud [1] and David Gagneul [1,*,†]

1 UMR Transfrontalière BioEcoAgro No. 1158, Univ. Lille, INRAE, Univ. Liège, UPJV, ISA, Univ. Artois, Univ. Littoral Côte d'Opale, ICV, SFR Condorcet FR CNRS 3417–Institut Charles Viollette, Joint Laboratory CHIC41H University of Lille-Florimond-Desprez, Villeneuve d'Ascq 59655, France
2 UMR Transfontalière BioEcoAgro No. 1158, Univ. Lille, INRAE, Univ. Liège, UPJV, ISA, Univ. Artois, Univ. Littoral Côte d'Opale, ICV, SFR Condorcet FR CNRS 3417-BIOlogie des Plantes et Innovation (BIOPI), Amiens 80025, France
3 Biomolécules et Biotechnologies Végétales, EA2106, Université de Tours, Tours 37200, France
4 UMR 1349 IGEPP, INRA, Agrocampus Ouest, Université de Rennes 1, Le Rheu 35650, France
5 Plateforme Analytique (PFA), Université de Picardie Jules Verne, Amiens 80039, France

*Author for correspondence: david.gagneul@univ-lille.fr
The authors contributed equally (G.B. and J.B.).
†Senior author

C.R. and D.G. designed the experiments. G.B., J.B., M.D., R.M., A.B., A.W., J.X.F., D.M., S. Ber., and S.Bas. performed the experiments and analyzed the data. G.B., R.M., D.M., and D.G. wrote the article and J.B., M.D., A.B., S.Bes., A.Q., J.L.H., and C.R. contribute to writing and revised the manuscript. D.G. supervised the project.
The author responsible for distribution of materials integral to the findings presented in this article in accordance with the policy described in the Instructions for Authors (https://academic.oup.com/plphys/pages/general-instructions) is David Gagneul (david.gagneul@univ-lille.fr).

Abstract

Fully substituted phenolamide accumulation in the pollen coat of Eudicotyledons is a conserved evolutionary chemical trait. Interestingly, spermidine derivatives are replaced by spermine derivatives as the main phenolamide accumulated in the Asteraceae family. Here, we show that the full substitution of spermine in chicory (*Cichorium intybus*) requires the successive action of two enzymes, that is spermidine hydroxycinnamoyl transferase-like proteins 1 and 2 (CiSHT1 and CiSHT2), two members of the BAHD enzyme family. Deletion of these genes in chicory using CRISPR/Cas9 gene editing technology evidenced that CiSHT2 catalyzes the first N-acylation steps, whereas CiSHT1 fulfills the substitution to give rise to tetracoumaroyl spermine. Additional experiments using *Nicotiana benthamiana* confirmed these findings. Expression of CiSHT2 alone promoted partially substituted spermine accumulation, and coexpression of CiSHT2 and CiSHT1 promoted synthesis and accumulation of the fully substituted spermine. Structural characterization of the main product of CiSHT2 using nuclear magnetic resonance revealed that CiSHT2 preferentially catalyzed N-acylation of secondary amines to form N^5,N^{10}-dicoumaroyl spermine, whereas CiSHT1 used this substrate to synthesize tetracoumaroyl spermine. We showed that spermine availability may be a key determinant toward preferential accumulation of spermine derivatives over spermidine derivatives in chicory. Our results reveal a subfunctionalization among the spermidine hydroxycinnamoyl transferase that

Received March 14, 2022. Accepted April 28, 2022. Advance access publication May 23, 2022

was accompanied by a modification of free polyamine metabolism that has resulted in the accumulation of this new phenolamide in chicory and most probably in all Asteraceae. Finally, genetically engineered yeast (*Saccharomyces cerevisiae*) was shown to be a promising host platform to produce these compounds.

Introduction

Plants accumulate a wide array of specialized metabolites. Historically defined as opposed to primary metabolites, these molecules have long been called secondary metabolites because they were often considered as evolutionary enigma or even waste products (Hartmann, 2007). Primary metabolites, that is, central metabolites, referred to molecules that are required for the survival of the host and which biosynthesis is fairly well conserved in all living organisms. Specialized metabolites include molecules that are dispensable for survival in an optimal environment but confer a great advantage in specific ecological niches and in the management of biological interactions (Pichersky and Lewinsohn, 2011). Therefore, their synthesis and accumulation are often distributed in a taxonomically restricted manner with few exceptions. These molecules are the basis of the extraordinary adaptability of plants to their environment as well as the remarkable chemical diversity occurring in the biosphere (Pichersky and Lewinsohn, 2011). Thus, terrestrialization of the green lineage is often associated with the emergence of these new molecules (Weng, 2014). They are involved in various ecological functions notably plant interaction with its environment, for example, pollinator attraction, symbiotic microorganism attraction, defense against pathogens and herbivores or environmental stresses (Ahmed et al., 2017). At the molecular level, the emergence of new metabolic pathways during plant evolution mainly relies on gene duplication followed by random mutations (Chae et al., 2014). These genetic events occurring in the open reading frames or/and in the regulatory parts of the genes can promote the appearance of new biochemical paths leading to new metabolites associated with new functions. This evolutionary scenario is called neofunctionalization if one gene retains its ancestral function, whereas the other evolves to promote a new function. If both genes experience mutations and participate in a new function while contributing together to the maintenance of their ancestral function, this is called subfunctionalization (Kroymann, 2011; Weng, 2014; Moghe and Last, 2015). Another model to explain the appearance of new metabolic pathways is escape from adaptive conflict (Kroymann, 2011; Moghe and Last, 2015). In this model, a single gene evolved a new function at the expense of the ancestral function. This gives rise to an adaptive conflict that is solved through gene duplication (Kroymann, 2011). In contrast to primary metabolism, in which selection results in enzymes with high efficiency and strict substrate specificity, enzymes from specialized metabolism usually have broad substrate specificity but low catalytic specificity, which favors the emergence of multiple new pathways during evolution (Weng et al., 2012). This enzymatic promiscuity is thought to play a central role in evolution of specialized metabolic enzymes and generation of chemical diversity (Weng et al., 2012).

Phenolics are specialized metabolites that are widely distributed in the plant kingdom and contribute to all aspects of plant life. They are mostly derived from the phenylpropanoid pathway. Products of this pathway, hydroxycinnamic acids, are recruited to form majority of phenolic compounds including lignin, tannins, suberin, and flavonoids. Hydroxycinnamic acid moieties, for example, coumaric, caffeic, ferulic acid, or sinapic acids are rarely accumulated under their free forms but are often conjugated to acid alcohols, sugars or amines to form esters, glycosides, or phenolamides, respectively. The latter are also termed phenylamides or hydroxycinnamic acid amides (Edreva et al., 2007; Roumani et al., 2021). These polyamine-derived molecules are mostly known for their involvement in floral induction or as defense compounds (Bassard et al., 2010; Roumani et al., 2021). Phenolic acids can be conjugated to either aromatic amines like tyramine, tryptamine, octopamine, or anthranilate or aliphatic polyamines like putrescine, spermidine, or spermine (Bassard et al., 2010; Roumani et al., 2021).

To date, all the enzymes involved in *N*-acylation of aliphatic polyamines belong to the superfamily of the BAHD acyltransferases (Roumani et al., 2021). For instance, agmatine coumaroyl transferase (ACT) catalyzes *N*-acylation of agmatine in barley (*Hordeum vulgare*) and Arabidopsis (*Arabidopsis thaliana*; Burhenne et al., 2003; Muroi et al., 2009), and hydroxycinnamoyl-CoA:putrescine acyltransferase (AT1) that of putrescine in *Nicotiana attenuata* (Onkokesung et al., 2012). The triamine spermidine was shown to be acylated by spermidine disinapoyl transferase (SDT) and spermidine dicoumaroyltransferase (SCT) in Arabidopsis (Luo et al., 2009), by hydroxycinnamoyl-CoA:spermidine acyltransferase (DH29) in *N. attenuata* (Onkokesung et al., 2012) and by spermidine hydroxycinnamoyl transferase (SHT) in the tapetal cells of Arabidopsis and apple (*Malus domestica*; Grienenberger et al., 2009; Elejalde-Palmett et al., 2015). We have previously identified and characterized two enzymes from chicory (*Cichorium intybus*), called spermidine hydroxycinnamoyl transferase-like proteins 1 and 2 (CiSHT1 and CiSHT2), closely related to AtSHT and MdSHT. Both chicory enzymes were shown to be involved in tetracoumaroyl spermine synthesis (Delporte et al., 2018). The only enzymes characterized so far that have the capability to acylate secondary amino groups to synthesize fully substituted polyamines are SHTs (Pichersky et al., 2006; Grienenberger et al., 2009; Elejalde-Palmett et al., 2015; Peng et al., 2016, 2019; Delporte et al., 2018; Perrin

et al., 2021). The accumulation of fully substituted spermidine derivatives was shown to be restricted to the pollen coat of Arabidopsis and apple tree and suggested as a marker of the pollen exine of Eudicotyledons (Grienenberger et al., 2009; Elejalde-Palmett et al., 2015). We provided evidence that spermine-derived phenolamides constitute a chemical signature of the pollen coat of the Asteraceae family (Delporte et al., 2018). Both enzymes identified in chicory acylated either spermine or spermidine in vitro in the presence of hydroxycinnamoyl-CoA and all intermediates were detected, but, surprisingly the fully substituted polyamines were not the major products. Additionally, heterologous expression of CiSHT2 in *sht* Arabidopsis mutants which do not accumulate phenolamide in the pollen coat led to similar inconsistency that is, some phenolamides were accumulated, but fully substituted phenolamides were not the main phenolamides (Delporte et al., 2018). Similar results were obtained when chicory hairy roots that did not accumulate phenolamides naturally were engineered to overexpress CiSHT2: no fully substituted phenolamides were detected whereas partially substituted phenolamides were present (Delporte et al., 2018). Moreover, heterologous and homologous expression of *CiSHT1* did not induce any phenolamide accumulation.

In this report, we conducted in planta experiments in order to clarify the roles of CiSHT1 and CiSHT2. In order to know if both enzymes were required for the production of tetracoumaroyl spermine in the tapetal cells, we generated chicory plants silenced in the expression of either *CiSHT1* or *CiSHT2* or both. Interestingly, *Cisht1* and *Cisht2* single mutant plants have a different flower bud phenolamide pattern than the wild-type (WT). *Cisht1* single mutant also exhibits a phenolamide profile different from that of the *Cisht2* mutant. The data suggest that both enzymes act sequentially in vivo to synthesize tetracoumaroyl spermine. Heterologous expression of these genes in *Nicotiana benthamiana* confirmed this assumption. We provided evidence that CiSHT2 acylates preferentially secondary amines using free or monoacylated polyamines as a substrate, whereas CiSHT1 uses the already acylated polyamines to produce fully substituted amines. Moreover, while this enzymatic system is able to acylate either spermine or spermidine in vivo and in vitro, further investigation suggested that free polyamine availability may contribute to direct the flux toward either spermidine or spermine derivative production. Additionally, a bioconversion system using yeast (*Saccharomyces cerevisiae*) as a chassis to produce spermine derivatives was successfully established but needs further improvement for the efficient production of different isomers of acylated spermine.

Results

Generation of *Cisht1* and *Cisht2* chicory mutants from genome-edited hairy roots

In order to decipher the functional roles of CiSHT1 and CiSHT2 and try to understand the meaning of this apparent biochemical redundancy, mutants have been generated. The genes *CiSHT1* and *CiSHT2* are 1,356-bp and 1,359-bp long, respectively, and do not contain any introns (Delporte et al., 2018). The target sequences were selected to induce breaks at positions 550 and 663 for *CiSHT1* and at positions 235 and 351 for *CiSHT2* (Figure 1A). Three binary vectors were prepared but only two gave rise to mutant plants (pYLCRISPR-sgRNA1–sgRNA2-CiSHT2 was ineffective). The first, named pYLCRISPR-sgRNA1–sgRNA2-CiSHT1, was designed to generate a double mutation in *CiSHT1* and the second, termed pYLCRISPR-sgRNA1–sgRNA2-SHT1/sgRNA1-sgRNA2-SHT2, to generate a double mutation in both genes, thus expressing four sgRNAs (Figure 1, B and C). Through *Agrobacterium rhizogenes*-mediated transformation, 12 and 7 glufosinate-resistant hairy root lines were obtained with pYLCRISPR-sgRNA1–sgRNA2-CiSHT1 and pYLCRISPR-sgRNA1–sgRNA2-SHT1/sgRNA1–sgRNA2-SHT2 vectors, respectively. Genomic DNA was extracted from each resistant line in order to determine the presence of mutations in the target *loci* by high-resolution melting (HRM) curve analysis. PCR products from plants with divergent melting curves compared to the WT, were further sequenced in order to confirm mutations and to characterize them. Seven lines with biallelic mutations for each transformation event have been identified and used for further experiments (Supplemental Figure S1). Three independent *sht1* mutant lines (8, 17, and 19; Supplemental Figure S1A) arising from transformation with pYLCRISPR-sgRNA1-sgRNA2-CiSHT1, three independent *sht2* mutant lines (21, 22, and 23; Supplemental Figure S1B), and one *sht1*/*sht2* double mutant line (7; Supplemental Figure S1C) arising from transformation with pYLCRISPR-sgRNA1–sgRNA2-SHT1/sgRNA1–sgRNA2-SHT2 were generated. Most of the mutations occurred at a position about 3-bp upstream the protospacer adjacent motif (PAM) sequence, as reported in other studies (Jinek et al., 2012). Editing types were either small deletion or insertions, but sometimes the inter-guide fragment was completely deleted as for the line SHT2 (23; Supplemental Figure S1B), which is consistent with what was shown in our previous study (Bernard et al., 2019). The target 1 of *CiSHT1* was not effective in editing the target sequence with both binary vectors. The fact that some targets are less effective than others was already observed in apple (Nishitani et al., 2013). The frame shifts induced by the genome-editing introduced an early stop on mRNA translation in all the mutated hairy root lines (Supplemental Figure S2).

Metabolic analysis of genome-edited plants

To investigate whether mutations generated by the CRISPR/Cas9 system had an impact on the phenolamide content of chicory flower buds, plants were regenerated from hairy roots. Flower buds from *sht1* mutant lines, *sht2* mutant lines, *sht1*/*sht2* double mutant line, and from plants transformed with *A. rhizogenes* WT strain (thereafter these plant lines are called WT) were collected. As shown previously (Delporte et al., 2018), tetracoumaroyl spermine was the main phenolamide in WT flower buds and both tricoumaroyl spermine and tricoumaroyl spermidine were

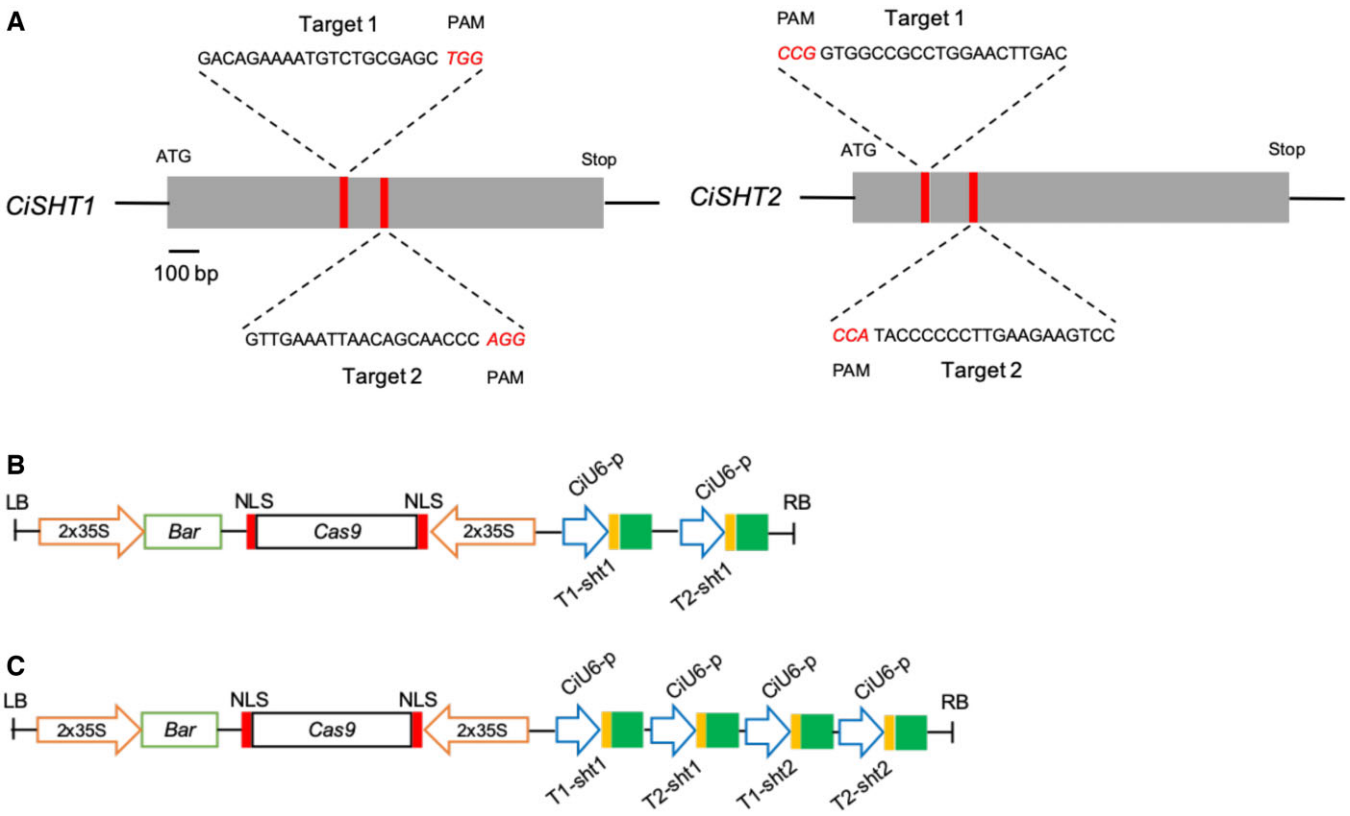

Figure 1 Schematic diagram of *CiSHT1* and *CiSHT2* gene structures and of vectors used to generate chicory mutants. A, Schematic diagram of *CiSHT1* and *CiSHT2* gene structures (gray rectangles) and target sequences (red lines). The translation initiation codon (ATG) and termination codon (stop) are shown. The target sequence is shown in capital letters, and the PAM sequence is marked in red. B and C, Schematic diagram of the pYLCRISPR-sgRNA1-sgRNA2-CiSHT1 and pYLCRISPR-sgRNA1-sgRNA2-SHT1/sgRNA1-sgRNA2-SHT2 vectors, respectively. Bar: Phosphinothricin acetyltransferase. 35S: cauliflower mosaic virus 35S promoter. NLS: nuclear localization sequence. CiU6-1P: *C. intybus* U6-1p promoter. LB: left border. RB: right border. T1 or T2 stands for target 1 or 2.

accumulated at a lower level (Figure 2). In the flower buds of *sht2* mutant lines and of the *sht1*/*sht2* double mutant, no phenolamides were detected and both genotypes exhibited identical metabolic profile (Figure 2). In the flower buds of the *sht1* mutant lines, only partially substituted spermine that is, dicoumaroyl spermine and tricoumaroyl spermine, were detected instead of tetracoumaroyl spermine. All together, these data suggest that both CiSHT1 and CiSHT2 are required to promote the synthesis of the fully substituted phenolamides in chicory flower buds. CiSHT2 would catalyze the first *N*-acylation steps, whereas CiSHT1 would fulfill the *N*-acylation to produce the fully substituted phenolamides.

Transient expression of *CiSHT1* and *CiSHT2* in *N. benthamiana* leaves

In order to confirm the previous results, *CiSHT1* and *CiSHT2* were transiently expressed in leaves of *N. benthamiana* where phenolamide-like compounds are not expected to accumulate. Leaves of *N. benthamiana* were infiltrated with *Agrobacterium tumefaciens* containing constructs of *CiSHT1* or *CiSHT2* or with a mixture of both strains. As a control, leaves were infiltrated with the void vector, pEAQ-HT. Four days after infiltration, leaves were collected, and the phenolic compounds were extracted before analysis. As expected, no spermine or spermidine derivatives were detected in *N. benthamiana* leaves infiltrated with bacteria containing either the empty vector, pEAQ-HT and more interestingly with the pEAQ-HT-DEST1-SHT1 (35S-CiSHT1) vector (Figure 3). In leaves transiently expressing *SHT2* (35S-CiSHT2), a mixture of phenolamides was detected, notably, mono- and di-coumaroyl spermidine as well as mono- and di-coumaroyl spermine. However, no fully substituted phenolamides could be detected or only in trace amounts. Finally, leaves agroinfiltrated with the vector pEAQ-HT-DEST1-SHT1 together with the vector pEAQ-HT-DEST1-SHT2 (35S-CiSHT1 + 35S-CiSHT2) accumulated tricoumaroyl spermidine, tricoumaroyl spermine, and tetracoumaroyl spermine. The main fully substituted phenolamide was tricoumaroyl spermidine (Figure 3). Interestingly, the peaks present in the chromatogram obtained with an extract of leaf infiltrated with pEAQ-HT-DEST1-SHT2 alone disappeared. To deepen our knowledge about the reaction catalyzed by both enzymes, an experiment was conducted in order to characterize the different isomers and determine their relative abundance. Eight independent *N. benthamiana* plants were agroinfiltrated as already described and the metabolite profiles analyzed by hierarchical clustering (Figure 4; Supplemental Table S1). Three monocoumaroyl spermidine

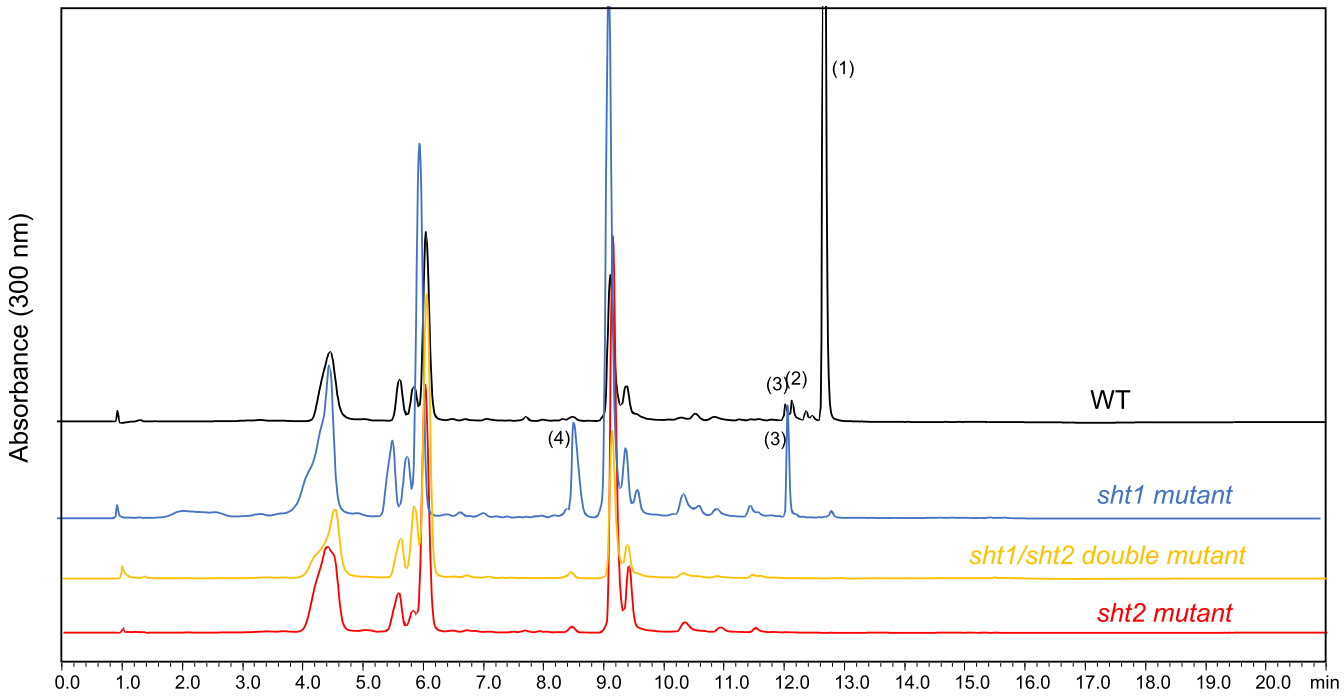

Figure 2 Stacked HPLC chromatograms of extracts obtained from flower buds at stages 13–15 isolated from WT, *sht1* mutant, *sht2* mutant or *sht1*/*sht2* mutant. The identity of the numbered peaks was confirmed by mass spectrometry: (1) tetracoumaroyl spermine, (2) tricoumaroyl spermidine, (3) tricoumaroyl spermine, and (4) dicoumaroyl spermine.

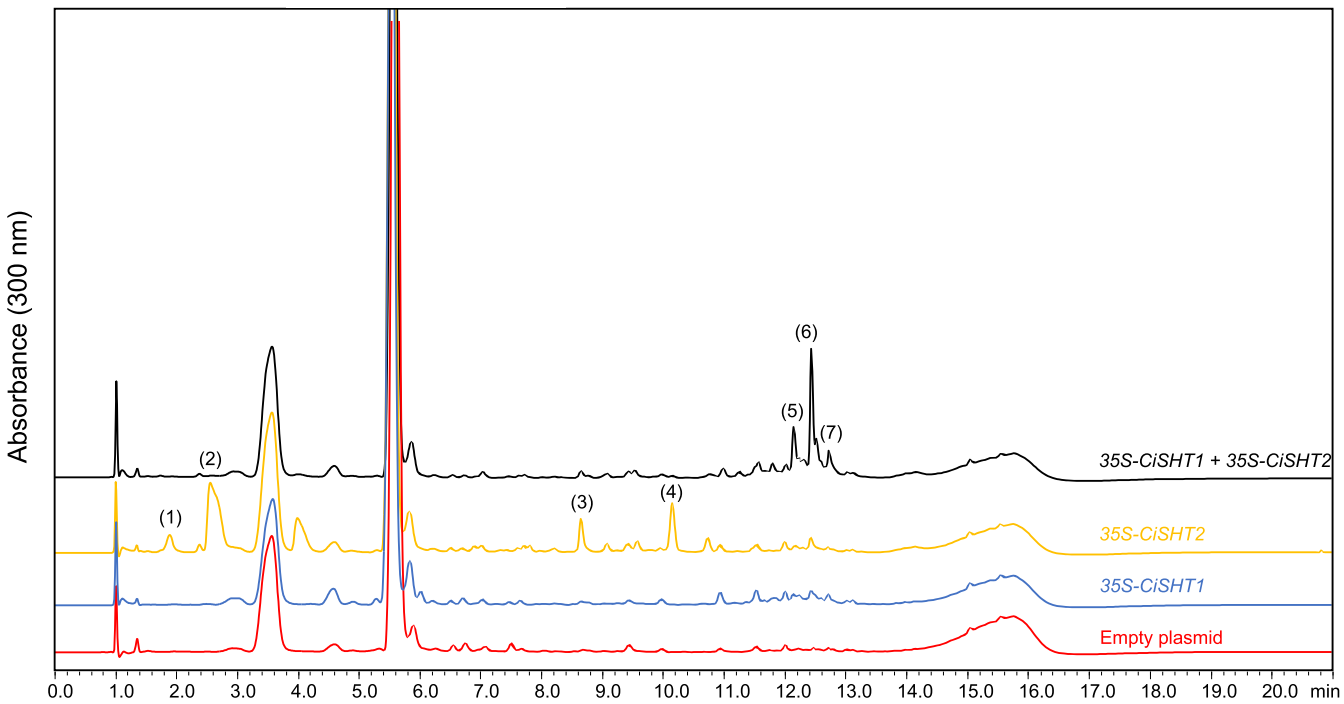

Figure 3 Stacked HPLC chromatograms of extracts obtained from agroinfiltrated *N. benthamiana* leaves. Plants were infiltrated with either the empty plasmid, *CiSHT1* (*35S-CiSHT1*), *CiSHT2* (*35S-CISHT2*), or *CiSHT1* plus *CiSHT2* (*35S-CiSHT1* + *35S-CiSHT2*). The identity of the numbered peaks was confirmed by mass spectrometry: (1) monocoumaroyl spermine, (2) monocoumaroyl spermidine, (3) dicoumaroyl spermine, (4) dicoumaroyl spermidine, (5) tricoumaroyl spermine, (6) tricoumaroyl spermidine, and (7) tetracoumaroyl spermine.

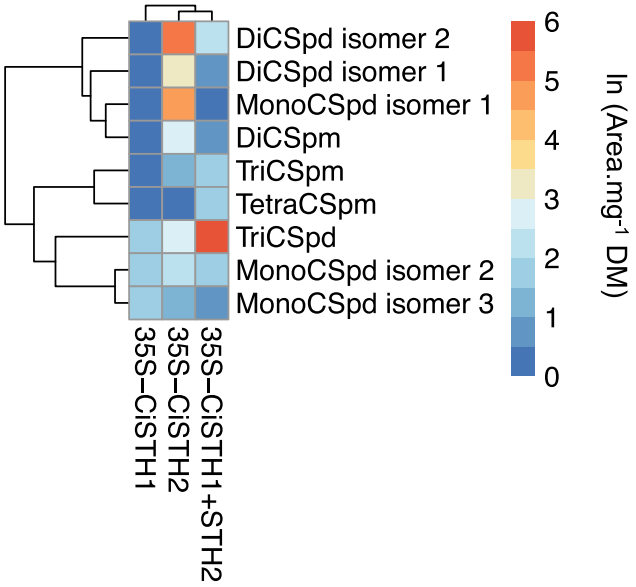

Figure 4 Heatmap of spermine and spermidine derived phenolamides in *N. benthamiana* agroinfiltrated with *CiSHT1*, *CiSHT2*, or *CiSHT1* plus *CiSHT2*. Pick area means for each condition (eight plants) and for each metabolite are expressed per mg of dry material (DM). Natural logarithm of the means for each condition was used to conduct the heatmap hierarchical clustering with the Ward's method. Colors in the heatmap are related to the sequential logarithmic scale presented in the right panel. DiCSpd, dicoumaroyl spermidine; MonoCSpd, monocoumaroyl spermidine; DiCSpm, dicoumaroyl spermine; TriCSpm, tricoumaroyl spermine; TetraCSpm, tetracoumaroyl spermine; TriCSpd, tricoumaroyl spermidine.

isomers, two dicoumaroyl spermidine isomers, and one dicoumaroyl spermine were detected when *N. benthamiana* leaves were agroinfiltrated with *CiSHT2*. Traces of tricoumaroyl spermidine were also detected. The main monocoumaroyl spermidine (MonoCSpd isomer 1) had a RT of 2.5 min in our chromatographic conditions (Figure 3) as also shown in our previous in vitro experiments (Delporte et al., 2018). It gave a $[M + H]^+$ ion at *m/z* 292.2013 as established by electrospray ionization high-resolution mass spectrometry (ESI-HRMS). Its molecular formula was determined to be $C_{16}H_{25}N_3O_2$ as expected for monocoumaroyl spermidine. ESI-MS-HRMS was performed to attempt to determine its precise structure. A previous study has shown that it was possible to distinguish the three regioisomers using this approach (Hu et al., 1996). Fragmentation pattern of each isomer was extensively examined by using either ^{15}N labeling or H/D exchange. Many fragments were common for all isomers but the relative intensity of the ions at *m/z* 218 and 221 were shown to be a diagnostic value. For N^1-monocoumaroyl spermidine, the ion at *m/z* 221 was more intense than that at *m/z* 218 whereas an opposite trend was observed for N^{10}-monocoumaroyl spermidine. The ion at *m/z* 221 was slightly more intense than the ion at *m/z* 218 for N^5-monocoumaroyl spermidine. Contribution of the ion at *m/z* at 221 for N^5-monocoumaroyl spermidine was attributed to an isomerization reaction responsible for the partial conversion of N^5-monocoumaroyl spermidine into N^1-monocoumaroyl spermidine. In our analysis, ESI-MS-HRMS spectra were similar to those reported by Hu et al. (1996) confirming identical behavior toward fragmentation of the isomers (Supplemental Figure S3). A structure has been assigned to the three isomers and N^5-monocoumaroyl spermidine was shown to be the main isomer accumulated in *N. benthamiana* leaves (MonoCSpd isomer 1; Supplemental Table S1). The identity of the two dicoumaroyl spermidine was not investigated further. Indeed it was already shown that their discrimination based on tandem mass spectrometry (MS/MS) data was not conclusive (Bigler et al., 1996). The main spermine-derived products accumulated in *N. benthamiana* leaves expressing *CiSHT2* (Figures 3 and 4; Supplemental Table S1) and accumulated in chicory *sht1* mutants (Figure 2) has a RT of 8.5 min in our chromatographic conditions. The same dicoumaroyl spermine isomer was synthesized by CiSHT2 in vitro as well as accumulated in chicory hairy roots overexpressing *CiSHT2* (Delporte et al., 2018). It was identified as one of the dicoumaroyl spermine isomers by mass spectrometry. This compound was purified from hairy root overexpressing *CiSHT2* and precisely characterized. The purified compound analyzed by ESI-HRMS gave a $[M + H]^+$ ion at *m/z* of 495.2971 and the molecular formula predicted from the accurate mass measurement was $C_{28}H_{38}N_4O_4$ as expected for a dicoumaroyl spermine isomer (Figure 5A). In addition, nuclear magnetic resonance (NMR) analysis revealed ^1H and ^{13}C characteristic signals consistent with a spermine derivative substituted with coumaroyl groups (Table 1; Supplemental Figure S4). It should be pointed out that the number of ^1H and ^{13}C signals observed on the spectra were surprisingly halved indicating a symmetry in the structure. Thus, spermine could be acylated either on N^1 and N^{14} positions or on N^5 and N^{10} positions. Long range ^1H-^{13}C correlations were investigated by 2D NMR using HMBC experiments to get more information about the connectivity of the coumaroyl groups on the spermine. $^3J_{HC}$ cross-peaks were observed between the protons H-4/H-11 (δ 3.57 ppm) and H-6/H-9 (δ 3.59 ppm) of the spermine and the equivalent quaternary carbons from coumaroyl groups (δ 169.9 ppm) corresponding to carbonyl of an amide function. These results suggest the grafting of coumaroyl units on secondary amines of spermine to give N^5, N^{10}-dicoumaroyl spermine (Figure 5C). In the ESI-HRMS spectrum, typical fragments were observed at *m/z* 147.0441, 204.1019, 275.1754, and 349.2600 confirming the identity of this compound (Figure 5, A and B). From the precursor ion at *m/z* 495.2709, a first loss of NH_3 (−17 Da) gave a fragment with a moderate intensity at *m/z* 478.2709. Loss of NH_3 from the ions at *m/z* 349.2600 and 275.1754 gave ions with very low intensities at *m/z* 332.2321 and 258.1490, respectively. All these NH_3 losses are in accordance with the presence of free primary amine functions in the dicoumaroyl spermine under investigation. Moreover, the very low intensity fragment at *m/z* 421.2117 confirm our structural determination. Indeed, it can only arise from the precursor ion at *m/z* 495.2709 by

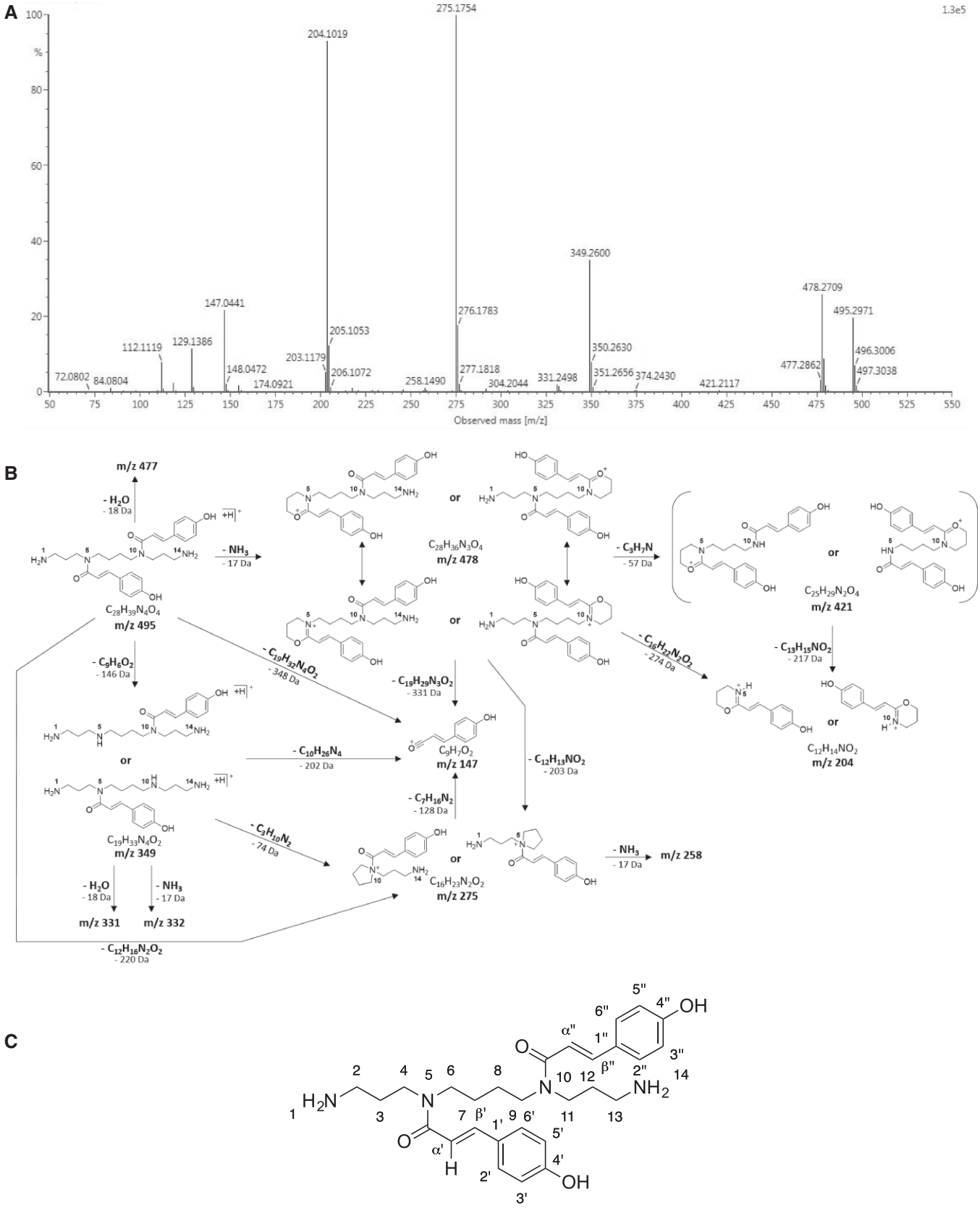

Figure 5 ESI-MS-HRMS spectra of purified N^5,N^{10}-dicoumaroyl spermine. A, Fragmentation of purified N^5,N^{10}- dicoumaroyl spermine. The position of the coumaroyl moieties was deduced from RMN data (see Table 1; Supplemental Figure S4). B, Fragmentation scheme of N^5,N^{10}-dicoumaroyl spermine. C, Chemical structure of N^5, N^{10}-dicoumaroyl spermine as deduced from NMR data.

Table 1 ^{1}H and ^{13}C-NMR data of N^5, N^{10}-dicoumaroyl spermine in methanol-d_4

Position	δ_C	δ_H (J in Hz)	HMBC
1	–	–	–
2	37.6	2.88 (t, J = 6.7)	3, 4
3	26.7	1.94 (t, J = 6.7)	2, 4
4	43.7	3.57 (m)	2, 3, 6
5	–	–	–
6	48.6	3.59 (m)	4, 8, CONH′
7	27.6	1.77 (m)	8, 9
8	27.6	1.77 (m)	4, 7
9	48.6	3.59 (m)	7, 11, CONH″
10	–	–	–
11	43.7	3.57 (m)	9, 12, 13
12	26.7	1.94 (t, J = 6.7)	11, 13
13	37.6	2.88 (t, J = 6.7)	11, 13
14	–	–	–
1′	127.4	–	3′, 5′, α′
2′	130.8	7.47 (d, J = 8.4)	4′, 6′, β′
3′	116.6	6.79 (d, J = 8.4)	1′, 4′, 5′
4′	160.8	–	–
5′	116.6	6.79 (d, J = 8.4)	1′, 3′, 4′
6′	130.8	7.47 (d, J = 8.4)	2′, 4′, β′
α′	113.8	6.87 (d, J = 15.7)	1′, CONH′
β′	145.0	7.59 (d, J = 15.7)	2′, 6′, α′, CONH′
CONH′	169.9	–	–
1″	127.4	–	3″, 5″, α″
2″	130.8	7.47 (d, J = 8.4)	4″, 6″, β″
3″	116.6	6.79 (d, J = 8.4)	1″, 4″, 5″
4″	160.8	–	–
5″	116.6	6.79 (d, J = 8.4)	1″, 3″, 4″
6″	130.8	7.47 (d, J = 8.4)	2″, 4″, β″
α″	113.8	6.87 (d, J = 15.7)	1″, CONH″
β″	145.0	7.59 (d, J = 15.7)	2″, 6″, α″, CONH″
CONH″	169.9	–	–

Position refers to the position indicated in Figure 5C. d, doublet; δ, chemical shift; HMBC, heteronuclear multiple bond correlation; J, coupling constant; m, other multiplet; t, triplet.

successive losses of NH_3 at one end and a propylamine chain at the other end (Figure 5B). To conclude, the main spermine synthesized by CiSHT2 in vitro as well as in vivo was N^5,N^{10}-dicoumaroyl spermine. It is tempting to assume that CiSHT2 would efficiently catalyze the *N*-acylation of secondary amines of spermine, while CiSHT1 would catalyze the *N*-acylation of primary amines of N^5, N^{10}-dicoumaroyl spermine. Production of tricoumaroyl spermine by CiSHT2 was effective but our data suggested that the capability of CiSHT2 to acylate the primary amine of dicoumaroyl spermine was less effective than that of CiSHT1.

Free polyamine availability controls the nature of the final product

While CiSHTs were shown in vitro to be able to catalyze spermidine and spermine *N*-acylation without apparent substrate preferences (Delporte et al., 2018), *N. benthamiana* and Arabidopsis transformed with the chicory SHTs mainly accumulates spermidine derivatives, whereas the main compound found in chicory flower buds is tetracoumaroyl spermine. This observation prompted us to determine whether the pools of available polyamines in a specific tissue could be responsible for the production of a particular compound rather than the acyl acceptor specificity of the enzymes. In Arabidopsis flower buds, the ratio of spermidine over spermine is clearly in favor of spermidine (around 5 times more spermidine than spermine; Fellenberg et al., 2012). We quantified free polyamines in chicory flower buds as well as in *N. benthamiana* leaves. In *N. benthamiana* leaves, spermidine levels (1 µmol.g^{-1} DW) were higher than that of spermine (0.12 µmol.g^{-1} DW). The ratio spermidine/spermine was close to 8. In contrast in chicory flower buds, this ratio was close to 0.8. Spermidine and spermine levels were 0.5 and 0.7 µmol.g^{-1} DW, respectively. These data suggest that the plant pool of available polyamine (and more specifically their relative abundance) likely plays a main role in determining SHTs product synthesis and accumulation.

Bioproduction of tetracoumaroyl spermine in *S. cerevisiae*

The elucidation of CiSHTs coordinated and sequential activities requirement for spermine derivative phenolamide synthesis prompted us to initiate metabolic engineering in yeast for the bioproduction of tetracoumaroyl spermine. To this aim, a precursor-directed synthesis strategy was employed. A yeast strain was first transformed with *At4Cl5* allowing CoA ester production from hydroxycinnamates added to the external medium as required for BAHD acyltransferases activities (Perrin et al., 2021). Then *CiSHT1* and *CiSHT2* alone or combined were introduced in the yeast chassis. The engineered yeasts were incubated on medium supplemented with coumarate. After 48 h, yeasts were pelleted, phenolic compounds extracted, and analyzed by liquid chromatography-ultraviolet (LC-UV) (Figure 6). As expected, no phenolamide could be detected when yeasts were transformed with *At4CL5* alone and in yeast coexpressing *At4CL5* and *CiSHT1*. In yeast transformed with *At4CL5* and *CiSHT2*, accumulations of monocoumaroyl spermidine and tricoumaroyl spermidine were evidenced. Partially substituted spermine derivatives was only effective when spermine was added. In *S. cerevisiae* grown in liquid medium, the spermidine/spermine ratio was shown to be around 6 (Marshall et al., 1979). Thus, the endogenous pools of spermidine were too important to support spermine-derived phenolamide production which confirms what was evidenced above, that is free polyamine pools determine the nature of the end product. When *At4CL5* and *CiSHT2* were coexpressed and yeasts incubated on medium supplemented with both coumarate and spermine, accumulation of monocoumaroyl spermine, dicoumaroyl spermine, and tricoumaroyl spermine occurred. In these conditions, yeasts accumulated also the spermidine derivatives but the main phenolamide was the N^1,N^5-dicoumaroyl spermine eluting at 8.5 min confirming the data presented above. Finally, as expected, the expression of *At4CL5*, *CiSHT2*, and *CiSHT1* together promotes accumulation of tetracoumaroyl spermine especially when coumarate and spermine were added in the medium. Identity of tetracoumaroyl

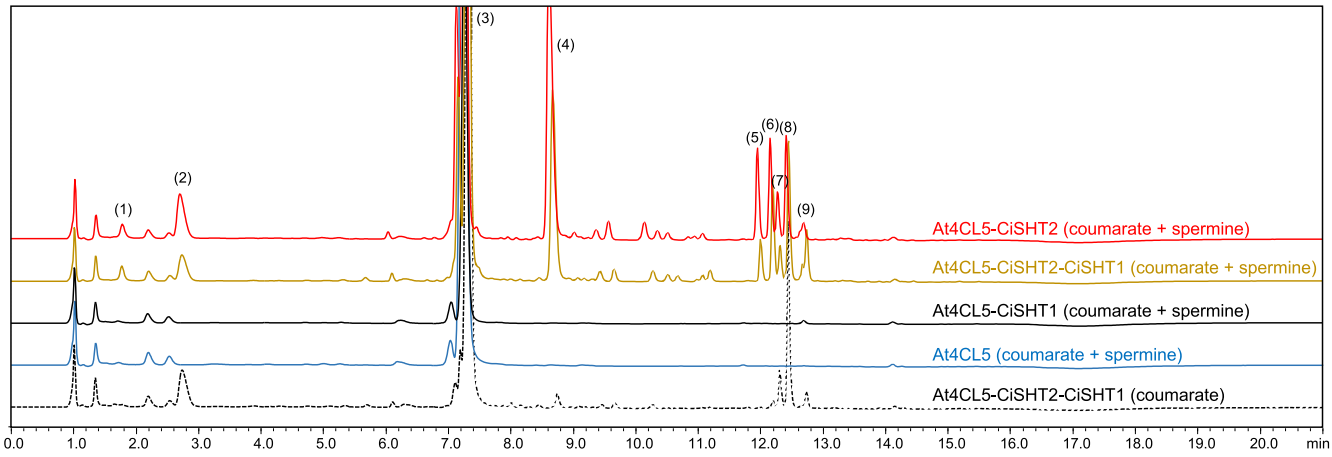

Figure 6 Stacked HPLC chromatograms of extracts from transgenic yeast expressing different combinations of genes. Yeasts were transformed with At4CL5 alone, with At4CL5 + CiSHT2 + CiSHT1, with At4CL5 + CiSHT1 or with At4CL5 + CiSHT2. The compounds added to the external medium are indicated in brackets. The identity of the numbered peaks was confirmed by mass spectrometry: (1) monocoumaroyl spermine, (2) monocoumaroyl spermidine, (3) coumarate, (4) dicoumaroyl spermine, (5) dihydrocoumaroyl dicoumaroyl spermine, (6) tricoumaroyl spermine, (7) dihydrocoumaroyl dicoumaroyl spermidine, (8) tricoumaroyl spermidine, and (9) tetracoumaroyl spermine. Tetracoumaroyl spermine coeluted with an unknown compound in our chromatographic conditions. Mass spectrometry analysis confirmed that tetracoumaroyl spermine was only present in yeast co-expressing both chicory genes (see Supplemental Figure S5).

spermine was confirmed by MS (Supplemental Figure S5). In these conditions partially acylated spermine derivative accumulation decreased accordingly, and accumulation of spermidine derivatives was also effective. Two additional peaks were detected when yeasts were engineered with *CiSHT2* or *CiSHT2* and *CiSHT1*. They correspond to a dihydrocoumaroyl spermidine derivative and a dihydrocoumaroyl spermine derivative (i.e. *N*-dihydrocoumaroyl, *N*′, *N*″-dicoumaroyl spermidine and *N*-dihydrocoumaroyl, *N*′, *N*″-dicoumaroyl spermine, Supplemental Figures S6 and S7). The yeast enoyl reductase TSC13 (temperature sensitive CSG2 suppressor protein 13) is known to reduce coumaroyl-CoA into dihydrocoumaroyl-CoA which is further used, in our case, as a substrate by CiSHTs and competed with coumaroyl-CoA (Perrin et al., 2021). This heterologous system confirms our findings, that is both enzymes are needed for tetracoumaroyl spermine accumulation in vivo and provide an efficient tool for the bioproduction of phenolamides derived either from spermidine or from spermine.

Discussion

The presence of fully substituted phenolamides in the outer surface of male gametophytes is a common feature in Eudicotyledons (Elejalde-Palmett et al., 2015). Two enzymes AtSHT and MdSHT belonging to the BAHD acyltransferases family were characterized and shown to be directly responsible for the synthesis of trisubstituted spermidine in the tapetum of anthers (Grienenberger et al., 2009; Elejalde-Palmett et al., 2015). Thereafter the synthesized compounds have to be exported out of the tapetal cells to be deposited on the pollen surface. The mechanism responsible for this deposition still needs to be described. A recent study has shown that in the Asteraceae family the major phenolamides found in the pollen wall are fully substituted spermine conjugates, and that the presence of these unusual compounds is linked to the activity of two new members of the SHT family in chicory: CiSHT1 and CiSHT2 (Delporte et al., 2018). The biochemical and functional characterization of these two enzymes has provided evidence of their involvement in the biosynthesis of tetracoumaroyl spermine. Nevertheless, in vitro and in vivo experiments suggested that there might be some particular features in the tapetum of chicory that act in favor of fully substituted spermine accumulation. Here, additional experiments were conducted to deepen our knowledge of this biochemical pathway.

The CRISPR/Cas9 system was used to knockout *CiSHT1* and *CiSHT2* using the protocol set up by Bernard et al. (2019). The metabolic analysis of mutant plants derived from transformed hairy roots has highlighted that both CiSHT1 and CiSHT2 are required and sufficient to promote tetracoumaroyl spermine biosynthesis in chicory. The *sht2* mutants did not produce phenolamides, whereas the *sht1* mutants only produced dicoumaroyl and tricoumaroyl spermine but not the fully acylated spermine. These data indicate a role for CiSHT2 in the first *N*-acylation steps and for CiSHT1 in the last steps. The results obtained with these mutants are in accordance with the experiments done with chicory hairy roots overexpressing either *CiSHT1* and *CiSHT2* (Delporte et al., 2018).

The requirement of both enzymes to synthesize the fully substituted phenolamides was further confirmed using *N. benthamiana* and yeast heterologous systems. Thus, no phenolamides were produced when expressing only *CiSHT1* while *CiSHT2* expression only promoted partially substituted spermine accumulation. The co-expression of both genes led to the expected fully acylated phenolamide synthesis and accumulation. The main molecule produced in vitro or in vivo by CiSHT2 is a dicoumaroyl spermine as determined by

mass spectrometry. To determine the preferred *N*-acylation sites of CiSHT2, this compound was purified and analyzed by NMR. It was identified as N^5,N^{10}-dicoumaroyl spermine. These data suggest that CiSHT2 may have a higher affinity for secondary amines of spermine and N^5- or N^{10}-monocoumaroyl spermine, whereas CiSHT1 would prefer primary amines of di- or tri-coumaroyl spermine.

Taken together these results suggest that CiSHT2 would more efficiently promote dicoumaroyl spermine synthesis, whereas CiSHT1 would perform the last *N*-acylation steps toward fully substituted amine biosynthesis. A similar biochemical mechanism was suggested in *N. attenuata* (Onkokesung et al., 2012). An acyltransferase (DH29) was shown to catalyze the first *N*-acylation step in dicaffeoyl spermidine formation, whereas a second enzyme named CV86 was suggested to act on monocaffeoyl spermidine synthesized by DH29 to promote diacylated spermidine synthesis. Position of caffeoyl moieties was not further investigated but both enzymes belong to the BAHD acyltransferase superfamily.

More detailed in vitro biochemical experiments are necessary to assess this assumption, but this task is hampered by the lack of commercial standards. Purification or chemical synthesis of these compounds may be considered but their high degree of diversity (number and position of substitutions and nature of the amines) and their low amounts in plant tissues render this work extremely challenging. Optimization of the yeast bioproduction system described in this study could help reaching this goal. The use of standards would also be of interest for absolute quantification and to confirm structure assignments. For this last point, very robust analytical experiments were conducted and we are therefore quite confident in our structure determination. For instance, for monocoumaroyl spermidine derivatives, ESI-MS-HRMS fragmentation patterns revealed to be very similar to those obtained with chemically synthesized standards (Hu et al., 1996). Likewise, for N^5, N^{10}-dicoumaroyl spermine, NMR evidenced unambiguously the grafting position of coumaroyl residues on secondary amines, the symmetry of the molecule being confirmed by the number of signals halved. Moreover, ESI-MS-HRMS fragmentation study was in agreement with this structural hypothesis. To conclude, ESI-MS-HRMS and NMR experiments conducted were proven to be very reliable analytical techniques for the structure assignments of spermine or spermine-derived phenolamides.

Recently an enzyme able to acylate spermine has been identified in *Solanum richardii*, a wild relative of eggplant (Peng et al., 2019). This enzyme named Spermine hydroxycinnamoyl transferase (SrSpmHT) was shown to use exclusively spermine as the acyl acceptor substrate and promote monohydroxycinnamoyl spermine synthesis. The product of the reaction was tentatively identified as N^1-coumaroyl spermine based on comparison with an authentic standard with LC-UV . Thus, SrSpmHT would acylate primary amine of spermine. SrSpmHT belongs to the BAHD family and is phylogenetically close to AtSDT and AtSCT and seems to have emerged and evolved independently of SHT family (Roumani et al., 2021). Like AtSDT and AtSCT, SrSpmHT lacks the FYGN motif, which was shown to be a specific motif in amino acid sequences of the enzymes belonging to the SHT family such as AtSHT, MdSHT, CiSHT1, and CiSHT2 (Delporte et al., 2018). Taken together, our data suggest that in chicory fully acylated spermine synthesis relies on a two-step mechanism. Furthermore, they confirm that the enzymes belonging to the SHT subfamily of the BAHD acyltransferase superfamily are the only enzymes identified to date, that are capable of acylating secondary amino groups of polyamines.

CiSHT1 and CiSHT2 are both able to use spermine or spermidine as acyl acceptors in vitro and in vivo. Nonetheless in chicory flower buds, the main phenolamide is tetracoumaroyl spermine. With no apparent preference for the substrate, it was tempting to assume that the supply of free polyamines could determine which phenolamide would be the main accumulated conjugate. It was shown that in Arabidopsis flower buds, the content of spermidine was 5 times higher than that of spermine (Fellenberg et al., 2012). We have previously shown that in *sht* Arabidopsis, mutant expressing *CiSHT2* in the tapetal cells, spermidine derivatives were the main phenolamides (Delporte et al., 2018). Furthermore, in *N. benthamiana* leaves transiently expressing *CiSHT1* and *CiSHT2* as well as in *S. cerevisiae* transformed with both genes, tricoumaroyl spermidine was the main product (this study). The measurement of free polyamines has shown that the ratio spermidine/spermine were 8 and 0.8 in *N. benthamiana* leaves and in chicory flower buds, respectively. This shows that substrate availability or substrate relative availability could determine the identity of the final product. This observation suggests that in the Asteraceae there are at least two evolutionary events that led to the accumulation of these unusual spermine derivatives in the pollen coat: modification of polyamine metabolism and modification of catalytic properties of BAHD-acyltransferases. An extended analysis of polyamine contents in species belonging to the Asteraceae family and close families may help to strengthen this hypothesis. It was previously shown that spermine conjugates were absent in Stylidiaceae, Argophyllaceae, and Calyceraceae (Delporte et al., 2018). This additional analysis should provide an overview of the chronology of the evolutionary events mentioned above. It will be interesting to decipher if modification of polyamine metabolism drove evolution of SHTs, if SHTs evolution led to polyamine metabolism changes or if both events occurred independently. Ultimately whatever the chain of events, this has led to metabolic diversification that could be responsible for an evolutionary advantage that still deserves to be uncovered. In any case, the functions of these fully acylated polyamines, deposited on the pollen surface, are still under debate, as is the benefit of accumulating spermine derivatives instead of spermidine derivatives. Many hypotheses have been made about

their biological roles (Grienenberger et al., 2009; Elejalde-Palmett et al., 2015; Vogt, 2018). The most obvious function of these compounds is the protection of male gametophytes harboring sperm cells (i.e. the cells responsible for transmitting half part of the genetic material to offspring) against UV radiation. It is possible that the advantage of switching from spermidine- to spermine-conjugates comes from the decoration of all the four nitrogen atoms of the spermine which increases the UV absorbance of a single molecule by about 30% compared to spermidine derivatives, without affecting the concentration of the metabolites, and therefore increases the protection capacity (Vogt, 2018). In Arabidopsis, the lack of phenolamides in the pollen coat was shown to have no effect on pollen viability or fertility (Grienenberger et al., 2009). Nevertheless, the impact of UV radiation on DNA has not been studied and it seems relevant to investigate UV damage at the molecular level. In this context, the analysis of pollen collected from the Arabidopsis *sht* mutant and the chicory *sht* double mutant compared to pollen collected from their WT counterparts could provide interesting clues. These compounds could also have some effect on plant interaction with pollinator (Lin and Mullin, 1999). Insect feeding studies using pollen collected from the mutants or from the WT could be considered. Moreover, the conjugates of hydroxycinnamic acids with polyamines have been proposed to have numerous biological activities such as, antifungal, antimicrobial, and antiviral effects (Walters et al., 2001; Fixon-Owoo et al., 2003; Kyselka et al., 2018).

The evaluation of biological activity is a difficult task due to the poor availability of pure compounds. The elucidation of the biochemical pathway of tetracoumaroyl spermine and its reconstruction in the heterologous system *S. cerevisiae*, implemented in this work, is an important step toward providing sufficient amounts of molecules to support these biological tests. Nevertheless, this bioproduction system still needs to be optimized to increase the production of spermine derivatives. Indeed, main compounds produced were not the fully substituted amines, and spermidine-derived compounds were the major products. Modification of polyamine metabolism toward spermine production may promote the synthesis of the spermine-derived phenolamides. In addition, the expected compounds were retained in the yeast intracellular medium, and catalytic constraints, such as feedback inhibition, may not favor the synthesis of the fully acylated compounds. The engineering of a strain secreting the final products in the culture media should be considered. It was recently shown that yeast could be a suitable host platform for the production and excretion of spermidine-derived phenolamides (Perrin et al., 2021). Finally, the catalytic versatility of the enzymatic system characterized in this study may be used to synthetize related bioactive compounds such as the kukoamines widely studied, among other, that possess numerous pharmacological effects, such as antihypertensive, anti-inflammatory, anti-analgesic, anti-sepsis, autoimmune-enhancing, and neuroprotective activities (Chantrapromma and Ganem, 1981; Wang et al., 2016; Li et al., 2017). Yeast expressing SHTs from different species was already exploited to produce spermidine acylated with dihydrocinnamic acids (Perrin et al., 2021). Our work showed that engineered yeast can also produce spermine acylated with dihydrocinnamic acids. An optimized yeast strain could result in kukoamines production and maybe tetradihydrocaffeic spermine, a compound still never synthetized and biologically assessed.

In summary, we have shown, through in vivo experiments, that CiSHT1 and CiSHT2 are both required for the synthesis of tetracoumaroyl spermine in chicory flower buds. We proposed that appearance of this phenolamide is based on two evolutionary events in chicory that is, modification of polyamine metabolism and gene duplication of an ancestral sht to give rise to subfunctionalization and appearance of a new metabolic pathway. In addition, we have generated two biological tools (chicory mutants and engineered yeasts) that could help to understand the in planta biological roles of phenolamides and facilitate their valorization in human uses.

Materials and methods

Plant material

Chicory (*C. intybus*) (L.) line "clone 17" (Florimond Desprez, Cappelle-en-Pévèle, France) as well as chicory hairy root lines overexpressing *CiSHT2* and plants regenerated from them (Delporte et al., 2018) were used in this study. Chicory and *N. benthamiana* plants were grown in a greenhouse under a 16-/8-h light/dark cycle. Hairy roots and plantlets regenerated from them were grown in a growth chamber (16-/8-h light/dark cycle at 25°C/20°C).

Design of sgRNA, construction of CRISPR/Cas9 vectors, and *A. rhizogenes* transformation

To introduce mutations in *CiSHT1* (GenBank accession MG457243.1) and *CiSHT2* (GenBank accession MG457244.1) coding sequences in order to knockout the genes, two guides RNAs have been designed for each gene according to their location in the gene and their GC content using the software crispor.tefor.net (Haeussler et al., 2016; Supplemental Figures S8 and S9). The four targets were chemically synthesized by SIGMA-ALDRICH (Gillingham, UK).

Primary vectors pKanCiU6-1p-sgRNA1-SHT1, pKanCiU6-1p-sgRNA2-SHT1, pKanCiU6-1p-sgRNA1-SHT2 and pKanCiU6-1p-sgRNA1-SHT2 containing the cassette "CiU6-1p-Guide-sgRNAscaffold" were constructed as previously described (Bernard et al., 2019). Binary vector pLYCRISPR-sgRNA1-sgRNA2-*CiSHT1* harboring the two sgRNAs and the *CAS9* was constructed as previously described (Bernard et al., 2019). To construct binary vectors expressing four sgRNAs (two sgRNAs targeting *SHT1* and two sgRNAs targeting *SHT2*), PCR using proofreading polymerase (PrimeStar HS DNA polymerase; TAKARA, Kasatu, Japan) with primary vectors as templates were run using the following primer pairs: GG1-F and GG1-R with pKanCiU6-1p-sgRNA1-SHT1, GG2-F and GG3-R with pKanCiU6-1p-sgRNA2-SHT1, GG3-F

and GG4-R with pKanCiU6-1p-sgRNA1-SHT2, and GG4-F and GG2-R with pKanCiU6-1p-sgRNA2-SHT2. The primer sequences are listed in Supplemental Table S2. The BsaI restriction site and the four nucleotides recombination sites for Golden Gate restriction/ligation method was added in the 5′-extremity of each primer. Then PCR products were purified with NucleoSpin Gel and PCR Clean-up kit (Macherey-Nagel, Düren, Germany) and were assembled with Golden Gate restriction/ligation method in pYLCRISPR/Cas9P35S-B as described by Ma and Liu (2016) to generate pYLCRISPR-sgRNA1-sgRNA2-*SHT1*/sgRNA1-sgRNA2-*SHT2* and pYLCRISPR-sgRNA1-sgRNA2-*CiSHT1*. The pYLCRISPR-sgRNA1-sgRNA2-*CiSHT2* was also generated but was not effective to generate mutants.

The *A. rhizogenes* strain 15834 (kindly provided by Marc Buée, INRAE, Nancy, France) was independently transformed by electroporation with the binary vectors as described elsewhere (Nagel et al., 1990).

Hairy root culture and selection and regeneration of plants

Hairy root induction was performed on leaves of "clone 17" using *A. rhizogenes* strains (WT or transformed with either pYLCRISPR-sgRNA1–sgRNA2-*CiSHT1* or pYLCRISPR-sgRNA1-sgRNA2-*SHT1*/sgRNA1-sgRNA2-*SHT2*) as described previously (Bernard et al., 2019). For selection of transformants, 10 mg.L^{-1} glufosinate–ammonium was added in the medium. Regenerated shoots were grown as previously described (Bernard et al., 2019). The well-developed plantlets were transferred to the greenhouse and grown until flowering. The regenerants exhibited a slightly modified phenotype. They had a characteristic hairy root syndrome phenotype, possessed wrinkled leaves and were smaller than WT plants. The regenerated plants did not need vernalization for flowering (Bogdanovic et al., 2014). Flower buds were harvested at developmental stages 13–15 when the phenolamide contents were shown to be the highest (Delporte et al., 2018). Samples were immediately immerged in liquid nitrogen and store at −80°C until use.

Genomic DNA extraction and HRM temperature analysis

Genomic DNA from hairy roots was extracted using the NucleoSpin Plant II kit (Macherey-Nagel, Düren, Germany) according to the manufacturer instructions. PCR was performed using Type-it HRM PCR (QIAGEN, Hilden, Germany) according to the manufacturer instructions. Twenty nanograms of genomic DNA were used as template for PCR. The primers used for the detection of gene editing events are listed in Supplemental Table S2 and were designed using Primer3 and Netprimer softwares. The PCR products were analyzed by HRM using Rotor-Gene 6000 cycler. Data were analyzed with Rotor Gene Q Serie software. Edited DNA fragments were amplified with primer pairs flanking the target regions (Supplemental Table S2). PCR products were analyzed by Sanger sequencing method and the chromatograms were analyzed with CodonCodeAligner software (Xing et al., 2014). Primer positions are indicated in Supplemental Figures S8 and S9.

Transient expression in *N. benthamiana*

Previously reported entry vectors pDONR207_SHT1 and pDONR207_SHT2 were used to generate expression vector for transient expression in *N. benthamiana* (Delporte et al., 2018). The open reading frames of *CiSHT1* and *CiSHT2* were introduced in pEAQ-HT-DEST1 vector by LR recombination to generate pEAQ-HT-DEST1-SHT1 and pEAQ-HT-DEST1-SHT2 (Sainsbury et al., 2009). The empty pEAQ-HT vector was used as a negative control. These three vectors were independently introduced in *A. tumefaciens* GV2260 by electroporation. Agrobacteria were grown and prepared for agroinfiltration as previously described (Legrand et al., 2016). For transformation, agrobacteria strains were prepared alone or mixed to reach a final optical density at 600nm (OD_{600}) of 0.8 (equal concentration of each strain). *Nicotiana benthamiana* was then infiltrated with strains harboring pEAQ-HT as a control, with pEAQ-HT-DEST1-SHT1 alone, with pEAQ-HT-DEST1-SHT2 alone or with a mixture of strains containing pEAQ-HT-DEST1-SHT1 or pEAQ-HT-DEST1-SHT2. Four to 6-week-old plants per combination were used. After 4 days, the infiltrated leaves were collected, immediately frozen in liquid nitrogen and stored at −80°C until use.

Expression in *S. cerevisiae*

The vectors pDRf1-4CL5-GW, pDRf1-4CL5, and pRS423-FjTAL were provided by Dominique Loqué (Eudes et al., 2011, 2016). pRS423-GW was generated by BP reaction with pRS423-FJTAL and pDONR221. pDONR-SHT1 and pDONR-SHT2 were used to generate pDRf1-4CL5-SHT2, pDRf1-4CL5-SHT1, and pRS423-SHT1 by LR recombination with pDRF1-4CL5-GW or pRS423-GW. The *S. cerevisiae pad1* knockout (*MATa his3Δ1 leu2Δ0 met15Δ0 ura3Δ0 Δ pad1*, ATCC 4005833) were transformed using the freeze–thaw method (Connelly et al., 1999; Gietz and Schiestl, 2007). Yeasts were selected on solid medium containing yeast nitrogen base (YNB) without amino acids supplemented with 2% glucose (w/v) and 1× dropout-uracil, 1× dropout-histidine, or 1× dropout-uracil–histidine. Overnight cultures from four independent single colonies of recombinant yeast harboring pDRf1-4CL5, pDRf1-4CL5-SHT2, pDRf1-4CL5-SHT1, or pDRf1-4CL5-SHT2 plus pRS423-SHT1 constructs were mixed and grown in 1× YNB medium supplemented with 2% glucose and the required yeast synthetic drop-out medium supplement. These cultures were used to inoculated 2 mL of fresh medium to reach an OD_{600} of 0.15. The liquid cultures were then incubated at 30°C at 200 rpm for 5 h before adding substrates. Coumarate, spermidine, and spermine were added at a final concentration of 1 mM. The cultures were further grown for 24 h at 200 rpm at 30°C in the presence or absence of the different precursors.

Plant phenolic acid extraction

For chicory and *N. benthamiana*, lyophilized plant material was powdered, and 25 mg were resuspended in 1 mL of a methanol/water/acetic acid mixture (75/23/2, v/v/v). The mixture was then incubated in the dark under agitation at 4°C for 1 h. Homogenate was clarified by centrifugation (14,000 *g*, 4°C, 10 min) and passed through a 0.45-µm filters. For *N. benthamiana* used for the statistical analysis, eight 4–6 week-old-plants per combination were used. Hundred milligrams of dry leaves were extracted for 10 min at 60°C under agitation (2,000 rpm) 4 times with 0.4 mL of hexane and finally 4 times with 0.4 mL of a mixture of water/methanol (1:1). The polar extract was diluted (1/10) before ESI-MS-HRMS analysis. For metabolite measurement of yeast, supernatant and pellet were separately collected by centrifugation (20,000 *g*, 5 min, 4°C). The supernatants were passed through a 0.45-µm filter prior to HPLC-UV analysis. The pellets were ground with glass beads in a mixture of methanol/water/acetic acid (75/23/2, v/v/v). Homogenates were clarified by centrifugation (14,000 *g*, 4°C, 10 min) and passed through a 0.45-µm filter before HPLC-UV analysis.

Metabolite analyses

Metabolite analysis by liquid chromatography-diode array detector (LC-DAD) was carried as described in Delporte et al. (2018). ESI-HRMS analysis, was performed according to the procedure described in our previous work (Delporte et al., 2018). For NMR analysis, pure compound was dissolved in 0.75 mL of solvent (methanol-d_4 or DMSO-d_6). Six hundred microliters of the solution were then transferred into a 5-mm NMR tube. NMR spectra were acquired at 300 K on a Bruker Avance III 600 spectrometer (600.13 MHz for proton frequencies, Wissembourg, France) equipped with a z-gradient inverse probe head (TXI, 5-mm tube). The TOPSPIN (V3.2; Bruker, Billerica, CA, USA) software was used. The 1D proton spectra were acquired using 32 scans of 128 K data points, using spectral widths of 8,403 Hz. The 1D carbon spectra were acquired using 24 K scans of 64 K data points, using spectral widths of 37,878 Hz. The 2D COSY and 2D TOCSY spectra were acquired using 8 scans per 256 increments that were collected into 2 K data points, using spectral widths of 12,019 Hz in both dimensions. For the TOCSY, a mixing time of 100 ms were employed. The NUS-based 2D HSQC (non uniform sampling-based 2D heteronuclear single quantum coherence) spectra were acquired using 16 scans per 8 K increments that were collected into 4 K data points, using spectral widths of 12,019 Hz in F2 and 26,412 Hz in F1. The NUS-based 2D HMBC spectra were acquired using 64 scans per 8 K increments that were collected into 4 K data points, using spectral widths of 12,019 Hz in F2 and 37,732 Hz in F1. The number of NUS sampling points was 256 complex points (3.125% sampling density of 8 K points; LeGuennec et al., 2015). All nonzero filled obtained spectra were manually phased and baseline-corrected, calibrated with solvent signal (^{1}H (3.31) and ^{13}C (49.0) for methanol-d_4; Fulmer et al., 2010).

Extraction and analysis of free polyamines

Polyamines were extracted and analyzed by liquid chromatography as described previously (Jubault et al., 2008). The HPLC design consisted of a thermoelectron pump (SpectraSystem P1000 XR, Thermo Fisher, San Jose, CA, USA) and (Spectra- Series AS100) autosampler with a 20-µL injection loop, and detection through an FP-2020 Plus fluorometer (Jasco, Inc., Easton, MD, USA). Signals were computed and analyzed using Azur software (Datalys, St Martin d'Hères, France).

Dicoumaroyl spermine purification

Hairy roots overexpressing *CiSHT2* generated in our previous study were used (Delporte et al., 2018). These lines were shown to accumulate high amounts of dicoumaroyl spermine when fed with exogenous spermine. Five grams of lyophilized material, cultivated as described, were powdered and extracted with 200 mL of a methanol/water/acetic acid mixture (75/23/2, v/v/v) for 2 h at 4°C in the dark under agitation. Homogenate was then clarified by centrifugation (5 min at 4,600 g) and the supernatant was passed through a 0.45-µm filter. The pellet was re-extracted a second time following the same procedure. Then, the filtrates were pooled and washed with ethyl-acetate (v/v) and the aqueous phase was collected and passed through a cation exchanger column (50 mg, CM-Sephadex C-50, PHARMACIA, Uppsala, Sweden) equilibrated with water. The resin was washed with 2 L of water and eluted with 20 mL of a mixture of methanol/8M acetic acid (v/v). The eluted fraction was concentrated under rotary evaporation to get a final volume of 1 mL. Dicoumaroyl spermine was purified after separation by HPLC using the protocol described above. The collected fractions containing dicoumaroyl spermine were then pooled and concentrated under rotary evaporation to reach a final volume of 2 mL. This concentrated fraction was further purified using a purify flash 4250_{250} (Interchim, Montluçon, France). Purification was performed on a 250 × 21 mm Interchrom 2 mm preparative column (RP18). The chromatographic separation was performed using water (solvent A) and methanol (solvent B), both acidified with 0.1% formic acid. The solvents were delivered at a flow rate of 22 mL.min^{-1}. The column was equilibrated with 20% solvent B. The separation conditions were as followed: start at 20% solvent B, 10 min gradient to 70% solvent B followed by 2 min gradient to 100%, and 3 min isocratic 100% solvent B, then a 2 min gradient to return to 20% solvent B and 5 min of isocratic re-equilibration at 20% solvent B. The collected fractions were concentrated under rotary evaporation. A 1-mL concentrated fraction was frozen and lyophilized in order to obtain a dried powder. Approximately 2.5 mg of dicoumaroyl spermine were purified by this procedure. The purified compound was analyzed by NMR and ESI-HRMS.

Statistical analysis

For heatmap construction, pick area for each quantification ion were evaluated and expressed per milligram of dry materials. Natural logarithm of the means for each condition

(eight plants) was used to conduct the heatmap hierarchical clustering with Ward's method. The heatmap was visualized using the pheatmap-package, R software (version 4.0.3, company Foundation for Statistical Computing, Vienna, Austria).

Accession numbers

Sequence data from this article can be found in the GenBank/EMBL data libraries under accession numbers MG457243 (CiSHT1) and MG457244 (CiSHT2).

Supplemental data

The following materials are available in the online version of this article.

Supplemental Table S1. Relative quantification of phenolamides in *N. benthamiana* agroinfiltrated with *CiSHT1*, *CiSHT2*, or *CiSHT1* + *CiSHT2*.

Supplemental Table S2. Sequence of primers used in this study.

Supplemental Figure S1. Genotypes of *sht1*, *sht2*, and *sht1*/*sht2* mutants.

Supplemental Figure S2. Predicted amino acid sequences of SHT1 and SHT2 of mutants used in this study.

Supplemental Figure S3. Characterization of monocoumaroyl spermidine isomers.

Supplemental Figure S4. ^{1}H NMR spectra of N^{5}, N^{10}-dicoumaroyl spermine.

Supplemental Figure S5. Extracted ion chromatograms and fragmentation of tetracoumaroyl spermine produced by engineered yeast.

Supplemental Figure S6. HRMS spectra in ESI^{+} of trisubstituted spermidine derivatives produced by engineered yeast recorded in HDMS^{E} mode.

Supplemental Figure S7. HRMS spectra in ESI^{+} of trisubstituted spermine derivatives produced by engineered yeast recorded in HDMS^{E} mode.

Supplemental Figure S8. *CiSHT1* DNA sequence, sgRNA target sites, and the primer sites for sequencing and HRM analysis.

Supplemental Figure S9. *CiSHT2* DNA sequence, sgRNA target sites, and the primer sites for sequencing and HRM analysis.

Acknowledgments

Authors would like to thank Professor George Iomonossof (John Innes Center) for providing the pEAQ vectors (pEAQ-HT and pEAQ-DEST1). This work has been performed using infrastructure and technical support of the Plateforme Serre, cultures et terrains expérimentaux-Université de Lille for the greenhouse.

Funding

G.B. and J.B. were supported by a doctoral fellowship from University of Lille and the Région Hauts-de-France, while M.D. was supported by a doctoral fellowship from the doctoral school 104 SMRE. This research was funded by an Alibiotech grant (2016-2020) obtained from the CPER/FEDER program. This study is part of the projects of the Chicory for One Health (CHIC41H) joint team between Florimond-Desprez and the University of Lille, funded by the European Union, and the European Regional Development Fund of the Region Hauts-de-France.

Conflict of interest statement. None declared.

References

Ahmed E, Arshad M, Zakriyya Khan M, Shoaib Amjad M, Mehreen Sadaf H, Riaz I, Sidra Sabir P, Ahmad N, Sabaoon P, Ejaz Ahmed P, et al. (2017) Secondary metabolites and their multidimensional prospective in plant life. J Pharmacogn Phytochem **6**: 205–214

Bassard JE, Ullmann P, Bernier F, Werck-Reichhart D (2010) Phenolamides: bridging polyamines to the phenolic metabolism. Phytochemistry **71**: 1808–1824

Bernard G, Gagneul D, dos Santos HA, Etienne A, Hilbert JL, Rambaud C (2019) Efficient genome editing using CRISPR/Cas9 technology in chicory. Int J Mol Sci **20**: 1155

Bigler L, Schnider CF, Hu W, Hesse M (1996) Acid-catalyzed isomerization of N,N′-Bis[(E)-3-(4-hydroxyphenyl)prop-2-enoyl]spermidines by the zip reaction. Helv Chim Acta **79**: 2152–2163

Bogdanovic MD, Todorovic SI, Banjanac T, Dragiƒáeviƒá MB, Verstappen FWA, Bouwmeester HJ, Simonoviƒá AD, Bogdanović MD, Todorović SI, Banjanac T, et al. (2014) Production of guaianolides in *Agrobacterium rhizogenes* - transformed chicory regenerants flowering in vitro. Ind Crops Prod **60**: 52–59

Burhenne K, Kristensen BK, Rasmussen SK (2003) A new class of N-hydroxycinnamoyltransferases: purification, cloning, and expression of a barley agmatine coumaroyltransferase (EC 2.3.1.64). J Biol Chem **278**: 13919–13927

Chae L, Kim T, Nilo-Poyanco R, Rhee SY (2014) Genomic signatures of specialized metabolism in plants. Science **344**: 510–3

Chantrapromma K, Ganem B (1981) Total synthesis of kukoamine A, an antihypertensive constituent of lycium chinense. Tetrahedron Lett **22**: 23–24

Connelly C, Dietrich F, Andre B, Dow S, Boeke J, Bakkoury M, Gentalen E, Foury F, Shoemaker D, Anderson K, et al. (1999) Functional characterization of the S. cerevisiae genome by gene deletion and parallel analysis. Science **285**: 901–906

Delporte M, Bernard G, Legrand G, Hielscher B, Lanoue A, Molinié R, Rambaud C, Mathiron D, Besseau S, Linka N, et al. (2018) A BAHD neofunctionalization promotes tetrahydroxycinnamoyl spermine accumulation in pollen coat of the Asteraceae family. J Exp Bot **69**: 5365–5371

Edreva AM, Velikova VB, Tsonev TD (2007) Phenylamides in plants. Russ J Plant Physiol **54**: 287–301

Elejalde-Palmett C, Dugé De Bernonville T, Glevarec G, Pichon O, Papon N, Courdavault V, St-Pierre B, Giglioli-Guivarc 'h N, Lanoue A, Besseau S (2015) Characterization of a spermidine hydroxycinnamoyltransferase in *Malus domestica* highlights the evolutionary conservation of trihydroxycinnamoyl spermidines in pollen coat of core Eudicotyledons. J Exp Bot **66**: 7271–7285

Eudes A, Baidoo EEK, Yang F, Burd H, Hadi MZ, Collins FW, Keasling JD, Loqué D (2011) Production of tranilast [N-(3′,4′-dimethoxycinnamoyl)- anthranilic acid] and its analogs in yeast *Saccharomyces cerevisiae*. Appl Microbiol Biotechnol **89**: 989–1000

Eudes A, Mouille M, Robinson DS, Benites VT, Wang G, Roux L, Tsai YL, Baidoo EEK, Chiu TY, Heazlewood JL, et al. (2016) Exploiting members of the BAHD acyltransferase family to synthesize multiple hydroxycinnamate and benzoate conjugates in yeast. Microb Cell Fact **15**: 198

Fellenberg C, Ziegler J, Handrick V, Vogt T (2012) Polyamine homeostasis in wild type and phenolamide deficient *Arabidopsis thaliana* stamens. Front Plant Sci **3**: 1–11

Fixon-Owoo S, Levasseur F, Williams K, Sabado TN, Lowe M, Klose M, Joffre Mercier A, Fields P, Atkinson J (2003) Preparation and biological assessment of hydroxycinnamic acid amides of polyamines. Phytochemistry **63**: 315–334

Fulmer GR, Miller AJM, Sherden NH, Gottlieb HE, Nudelman A, Stoltz BM, Bercaw JE, Goldberg KI (2010) NMR chemical shifts of trace impurities: common laboratory solvents, organics, and gases in deuterated solvents relevant to the organometallic chemist. Organometallics **29**: 2176–2179

Gietz RD, Schiestl RH (2007) Quick and easy yeast transformation using the LiAc/SS carrier DNA/PEG method. Nat Protoc **2**: 35–37

Grienenberger E, Besseau SS, Geoffroy P, Debayle D, Heintz D, Lapierre C, Pollet B, Heitz T, Legrand M (2009) A BAHD acyltransferase is expressed in the tapetum of Arabidopsis anthers and is involved in the synthesis of hydroxycinnamoyl spermidines. Plant J **58**: 246–259

Haeussler M, Schönig K, Eckert H, Eschstruth A, Mianné J, Renaud J, Schneider-maunoury S, Shkumatava A, Teboul L, Kent J, et al. (2016) Evaluation of off-target and on-target scoring algorithms and integration into the guide RNA selection tool CRISPOR. Genome Biol **17**: 148

Hartmann T (2007) From waste products to ecochemicals: fifty years research of plant secondary metabolism. Phytochemistry **68**: 2831–2846

Hu W, Reder E, Hesse M (1996) Neighboring-group participation in the mass-spectral decomposition of 4-hydroxycinnamoyl-spermidines. Helv Chim Acta **79**: 2137–2151

Jinek M, Chylinski K, Fonfara I, Hauer M, Doudna JA, Charpentier E (2012) A programmable dual-RNA-guided DNA endonuclease in adaptive bacterial immunity. Science **337**: 816–821

Jubault M, Hamon C, Gravot A, Lariagon C, Delourme R, Bouchereau A, Manzanares-Dauleux MJ (2008) Differential regulation of root arginine catabolism and polyamine metabolism in clubroot-susceptible and partially resistant arabidopsis genotypes. Plant Physiol **146**: 2008–2019

Kroymann J (2011) Natural diversity and adaptation in plant secondary metabolism. Curr Opin Plant Biol **14**: 246–251

Kyselka J, Bleha R, Dragoun M, Bialasová K, Horáčková Š, Schätz M, Sluková M, Filip V, Synytsya A (2018) Antifungal polyamides of hydroxycinnamic acids from sunflower bee pollen. J Agric Food Chem **66**: 11018–11026

Legrand G, Delporte M, Khelifi C, Harant A, Vuylsteker C, Mörchen M, Hance P, Hilbert J-L, Gagneul D (2016) Identification and characterization of five BAHD acyltransferases involved in hydroxycinnamoyl ester metabolism in chicory. Front Plant Sci **7**: 741

LeGuennec A, Dumez J-N, Giraudeau P, Caldarelli S (2015) Resolution-enhanced 2D NMR of complex mixtures by non-uniform sampling. Magn Reson Chem **53**: 913–920

Li G, Zhou F, Chen Y, Zhang W, Wang N (2017) Kukoamine A attenuates insulin resistance and fatty liver through downregulation of Srebp-1c. Biomed Pharmacother **89**: 536–543

Lin S, Mullin CA (1999) Lipid, polyamide, and flavonol phagostimulants for adult western corn rootworm from sunflower (Helianthus annuus L.) pollen. J Agric Food Chem **47**: 1223–1229

Luo J, Fuell C, Parr A, Hill L, Bailey P, Elliott K, Fairhurst SA, Martin C, Michael AJ (2009) A novel polyamine acyltransferase responsible for the accumulation of spermidine conjugates in Arabidopsis seed. Plant Cell **21**: 318–333

Ma X, Liu Y (2016) CRISPR/Cas9-based multiplex genome editing in monocot and dicot plants. Curr Protoc Mol Biol **115**: 31.6.1–31.6.21

Marshall M, Russo G, Van Etten J, Nickerson K (1979) Polyamines in dimorphic fungi. Curr Microbiol **2**: 187–190

Moghe GD, Last RL (2015) Something old, something new: conserved enzymes and the evolution of novelty in plant specialized metabolism. Plant Physiol **169**: 1512–1523

Muroi A, Ishihara A, Tanaka C, Ishizuka A, Takabayashi J, Miyoshi H, Nishioka T (2009) Accumulation of hydroxycinnamic acid amides induced by pathogen infection and identification of agmatine coumaroyltransferase in *Arabidopsis thaliana*. Planta **230**: 517–527

Nagel R, Elliot A, Masel A, Birch RG, Manners JM (1990) Electroporation of binary Ti plasmid vector into Agrobacterium tumefaciens and *Agrobacterium rhizogenes*. FEMS Microbiol Lett **67**: 325–328

Nishitani C, Hirai N, Komori S, Wada M, Kazuma O (2013) Efficient genome editing in apple using a CRISPR/Cas9 system. Sci Rep **6**: 31481

Onkokesung N, Gaquerel E, Kotkar H, Kaur H, Baldwin IT, Galis I (2012) MYB8 controls inducible phenolamide levels by activating three novel hydroxycinnamoyl-coenzyme A: polyamine transferases in *Nicotiana attenuata*. Plant Physiol **158**: 389–407

Peng H, Meyer RS, Yang T, Whitaker BD, Trouth F, Shangguan L, Huang J, Litt A, Little DP, Ke H, et al. (2019) A novel hydroxycinnamoyl transferase for synthesis of hydroxycinnamoyl spermine conjugates in plants. BMC Plant Biol **19**: 1–13

Peng H, Yang T, Whitaker BD, Trouth F, Shangguan L, Dong W, Jurick WM (2016) Characterization of spermidine hydroxycinnamoyl transferases from eggplant (Solanum melongena L.) and its wild relative *Solanum richardii* Dunal. Hortic Res **3**: 1–9

Perrin J, Kulagina N, Unlubayir M, Munsch T, Carqueijeiro I, Dugé de Bernonville T, De Craene JO, Clastre M, St-Pierre B, Giglioli-Guivarc'h N, et al. (2021) Exploiting Spermidine N-HydroxycinnamoylTransferase diversity and substrate promiscuity to produce various tri-hydroxycinnamoyl spermidines and analogs in engineered yeast. ACS Synth Biol **10**: 286–296

Pichersky E, Lewinsohn E (2011) Convergent evolution in plant specialized metabolism. Annu Rev Plant Biol **62**: 549–566

Pichersky E, Noel JP, Dudareva N (2006) Biosynthesis of plant volatiles: nature's diversity and ingenuity. Science **311**: 808–811

Roumani M, Besseau S, Gagneul D, Robin C, Larbat R (2021) Phenolamides in plants: an update on their function, regulation, and origin of their biosynthetic enzymes. J Exp Bot **72**: 2334–2355

Sainsbury F, Thuenemann EC, Lomonossoff GP (2009) pEAQ: versatile expression vectors for easy and quick transient expression of heterologous proteins in plants. Plant Biotechnol J **7**: 682–693

Vogt T (2018) Unusual spermine-conjugated hydroxycinnamic acids on polle: function and evolutionary advantage. J Exp Bot **69**: 5311–5318

Walters D, Meurer-Grimes B, Rovira I (2001) Antifungal activity of three spermidine conjugates. FEMS Microbiol Lett **201**: 255–258

Wang Q, Li H, Sun Z, Dong L, Gao L, Liu C, Wang X (2016) Kukoamine A inhibits human glioblastoma cell growth and migration through apoptosis induction and epithelial-mesenchymal transition attenuation. Sci Rep **6**: 36543

Weng J (2014) The evolutionary paths towards complexity: a metabolic perspective. New Phytol **201**: 1141–1149

Weng J, Philippe RN, Noel JP, Weng JK, Philippe RN, Noel JP (2012) The rise of chemodiversity in plants. Science **336**: 1667–1670

Xing HL, Dong L, Wang ZP, Zhang HY, Han CY, Liu B, Wang XC, Chen QJ (2014) A CRISPR/Cas9 toolkit for multiplex genome editing in plants. BMC Plant Biol **14**: 327